



# Simulating Wave Climate in the Salish Sea

**September 2018**

Zhaoqing Yang  
Taiping Wang  
Gabriel García-Medina

Wei-Cheng Wu  
Luca Castrucci

## DISCLAIMER

This report was prepared as an account of work sponsored by an agency of the United States Government. Neither the United States Government nor any agency thereof, nor Battelle Memorial Institute, nor any of their employees, makes **any warranty, express or implied, or assumes any legal liability or responsibility for the accuracy, completeness, or usefulness of any information, apparatus, product, or process disclosed, or represents that its use would not infringe privately owned rights.** Reference herein to any specific commercial product, process, or service by trade name, trademark, manufacturer, or otherwise does not necessarily constitute or imply its endorsement, recommendation, or favoring by the United States Government or any agency thereof, or Battelle Memorial Institute. The views and opinions of authors expressed herein do not necessarily state or reflect those of the United States Government or any agency thereof.

PACIFIC NORTHWEST NATIONAL LABORATORY  
*operated by*  
BATTELLE  
*for the*  
UNITED STATES DEPARTMENT OF ENERGY  
*under Contract DE-AC05-76RL01830*

## Preface

This study has been funded wholly or in part by the U.S.s Environmental Protection Agency under assistance agreement PC-01J22301 through the Washington Department of Fish and Wildlife, as part of the Planning for Sea Level Rise in Puget Sound: Guidelines, Mapping, and Waves project led by the Climate Impact Group of the University of Washington. The Weather Research and Forecasting climate simulation was supported by the Strategic Environmental Research and Development Program under Contract RC-2546 and by the U.S. Department of Energy, Office of Energy Efficiency and Renewable Energy, Water Power Technologies Office. The wave model simulation was performed using the facilities of the Pacific Northwest National Laboratory's Institutional Computing Center.

Suggested Citation: Yang Z, W-C Wu, T Wang, L Castrucci, and G García-medina. 2018. Simulating Wave Climate in the Salish Sea. PNNL-27998, Pacific Northwest National Laboratory, Richland, Washington.

## Abbreviations and Acronyms

CFSR	Climate Forecast System Reanalysis
NCEP	National Centers for Environmental Prediction
NOAA	National Oceanic and Atmospheric Administration
PE	percent error
PNNL	Pacific Northwest National Laboratory
RMSE	root-mean-square-error
SI	scatter index
UnSWAN	Unstructured-grid Simulating WAVes Nearshore
WRF	Weather Research and Forecasting
WWIII	WaveWatchIII

# Contents

Preface .....	iii
Abbreviations and Acronyms .....	iv
1.0 Introduction .....	1
2.0 Methodology.....	1
2.1 Model Setup .....	1
2.2 Wind Forcing .....	3
2.3 Simulation Period.....	5
3.0 Model Results.....	6
3.1 Model Validation – Time History .....	6
3.2 Model Validation – Error Statistics.....	10
3.3 Wave Climate.....	10
4.0 Summary.....	12
5.0 References .....	13
Appendix A – Formulations of the Error Statistic Parameters .....	A.1
Appendix B – Data File Format.....	B.1

## Figures

Figure 1. West Coast regional WWIII model domains and Salish Sea UnSWAN model domain. ....	2
Figure 2. UnSWAN model grid for the Salish Sea .....	3
Figure 3. Comparison of NOAA NCEP CFSR and PNNL WRF model grid resolutions .....	4
Figure 4. Scatter plots of hourly CFSR wind and WRF wind against observed data at Buoy 46088 in the eastern Strait of Juan de Fuca .....	5
Figure 5. Scatter plots of hourly CFSR wind and WRF wind against observed data at Buoy 46131, in the northern Georgia Strait .....	5
Figure 6. Comparison of the hourly wave climate at Buoys 46087, 46088, 46146, and 46131 for the simulation period (2011–2015) and data record period.....	6
Figure 7. Comparison of simulated and measured hourly significant wave height at Buoys 46087 and 46088 in the Strait of Juan de Fuca and Buoys 46146 and 46131 in the Georgia Strait for 2015.....	7
Figure 8. Scatter plots of modeled and observed significant wave heights at hourly intervals at Buoys 46087, 46088, 46146, and 46131 for the period of 2011–2015 .....	8
Figure 9. Comparison of simulated and measured peak period at Buoys 46087 and 46088 for 2015.....	9
Figure 10. Scatter plots of modeled and observed wave peak period at hourly intervals at Buoys 46087 and 46088 for the period of 2011–2015.....	9
Figure 11. Distribution of significant wave height on December 11, 2015 .....	11
Figure 12. Comparison of significant wave height at Neah Bay and Seattle.....	11
Figure 13. Simulated 1% significant wave height and corresponding peak period and direction based on hourly output of five years of simulation (2011–2015).....	12

## Tables

Table 2.1. Summary of nested WWIII model grids.....	1
Table 3.1. Error statistics of simulated $H_s$ and $T_p$ .....	10

# 1.0 Introduction

Large waves and storm surges induced by extreme weather events pose great risk to coastal communities. The Pacific Northwest coast is among the top wave resource regions of U.S. coastal regions, based on the first wave resource assessment study conducted by the Electric Power Research Institute, Inc. (EPRI 2011). However, based on a literature review, no detailed modeling studies have been conducted to simulate the wave climate in the Salish Sea and to understand how remote swells in the Pacific Ocean propagate into the Salish Sea. There are also very limited wave measurements within the Salish Sea that have high-quality spectral data. Therefore, there is a strong need to conduct high-resolution wave modeling to understand the wave climate and estimate the maximum wave heights in the Salish Sea, especially within the complex sub-basins of Puget Sound.

# 2.0 Methodology

The methodology involved model grid development, specification of model boundary conditions and model parameters configuration for simulating wave growth and propagation in the Salish Sea.

## 2.1 Model Setup

This study followed the same modeling approach described by Yang et al. (2017, 2018). The approach consists of two modeling components: 1) a global-regional, nested-grid WaveWatchIII (WWIII) model to provide open boundary conditions and 2) a high-resolution unstructured-grid Simulating WAVes Nearshore (UnSWAN) model to simulate wave climate in the Salish Sea. Three levels of nested grids with WWIII were set up to simulate wave climate from global to regional scales. The WWIII model grid configurations are shown in Table 2.1. The West Coast regional WWIII model domains for level 2 (L2) and level 3 (L3) nested grids are shown in Figure 1.

**Table 2.1.** Summary of nested WWIII model grids.

Grid Name	Coverage	Resolution (long × lat)
Global Grid L1	77.5°S – 77.5°N; 0 – 360°W	0.5° × 0.5°
Nested Grid L2	28.5° – 50.5°N; 132° – 113.5°W	0.1° × 0.1° (6' × 6')
Nested Grid L3	30.5° – 49.5°N; 128° – 115.5°W	1' × 1'

The UnSWAN model domain covers the entire Salish Sea, including the Strait of Juan de Fuca, Strait of Georgia, and Puget Sound, as shown in Figure 2. The unstructured Salish Sea model grid consists of approximately 120,000 nodes and 217,000 elements, with a grid cell resolution of about 8 km along the open boundary to an average of 200 m inside Puget Sound.

The model was run in non-stationary mode with a time step of 10 minutes. The wave spectrum was discretized in frequency space using 29 logarithmically spaced bins from 0.035 to 0.505 Hz. In directional space 24 equally spaced bins are specified with a directional resolution of 15 degrees.

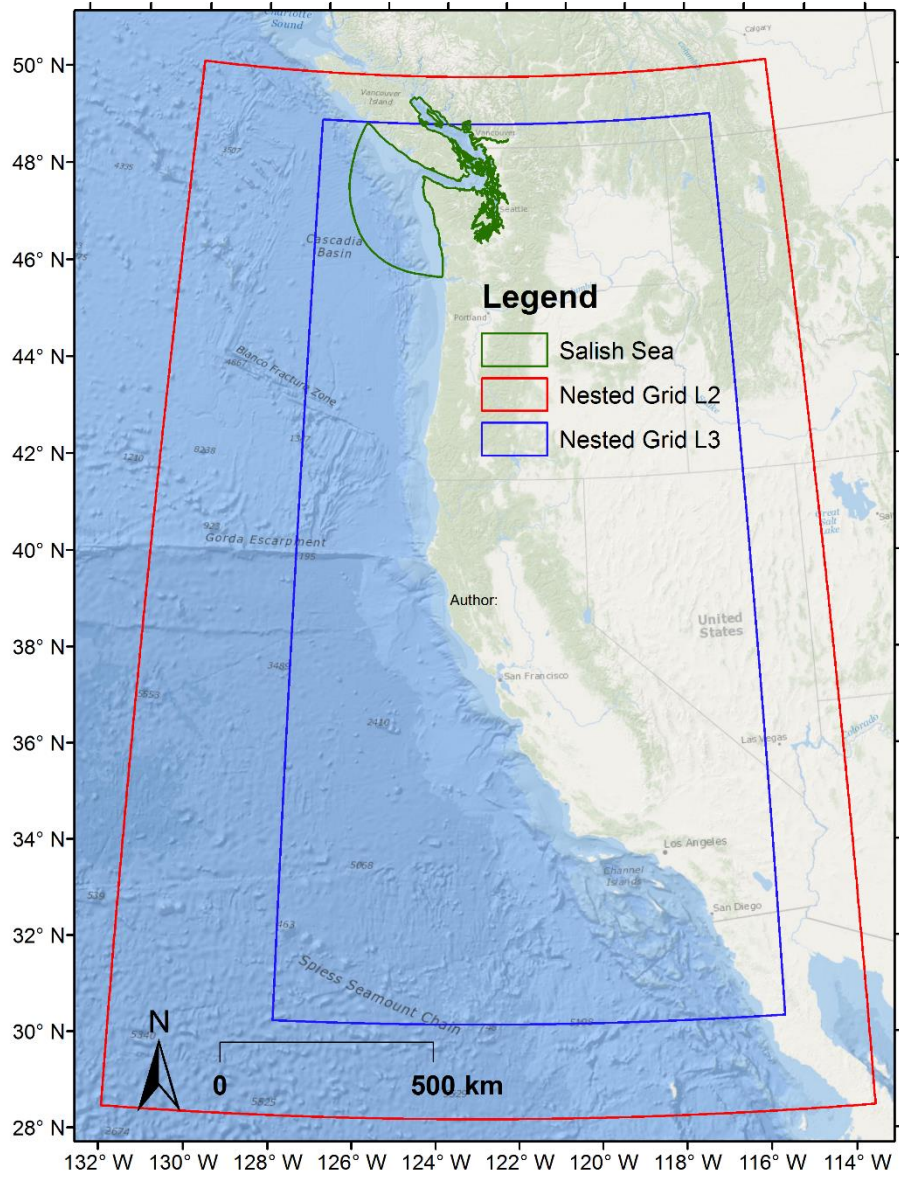


**Figure 1.** West Coast regional WWIII model domains and Salish Sea UnSWAN model domain.





**Figure 2.** UnSWAN model grid for the Salish Sea.

## 2.2 Wind Forcing

Sea surface wind is the most important forcing mechanism in simulating wave growth and propagation. In this study, the National Oceanic and Atmospheric Administration’s (NOAA’s) National Centers for Environmental Prediction (NCEP) Climate Forecast System Reanalysis (CFSR) wind was used to drive the WWIII simulation. The CFSR wind has a 0.5 degree spatial resolution and an hourly temporal resolution. While this is sufficient for the regional wave modeling using WWIII, it does not have the resolution required for the UnSWAN Salish Sea model simulation. To drive the UnSWAN Salish Sea model, we used wind fields from a high-resolution Weather Research and Forecasting (WRF) model simulation generated by PNNL (Gao et al. 2017). The PNNL WRF simulation covers the western U.S. at a grid resolution of 6 km, for the period of 1980–2015. Model solutions for wave bulk parameters, including significant wave height, peak wave period, and direction are outputted at hourly intervals. Comparison of NCEP CFSR and PNNL WRF model grid resolutions are provided in Figure 3.

Comparisons of hourly CFSR and WRF winds with observed data at Buoy 46088 in the Strait of Juan de Fuca and Buoy 46131 in the Strait of Georgia are shown in Figure 4 and Figure 5, respectively. The comparisons suggest that the WRF wind is more accurate in the Salish Sea than the CFSR wind, likely



due to the finer grid resolution. In general, CFSR tends to under-predict the sea surface wind in the Salish Sea.

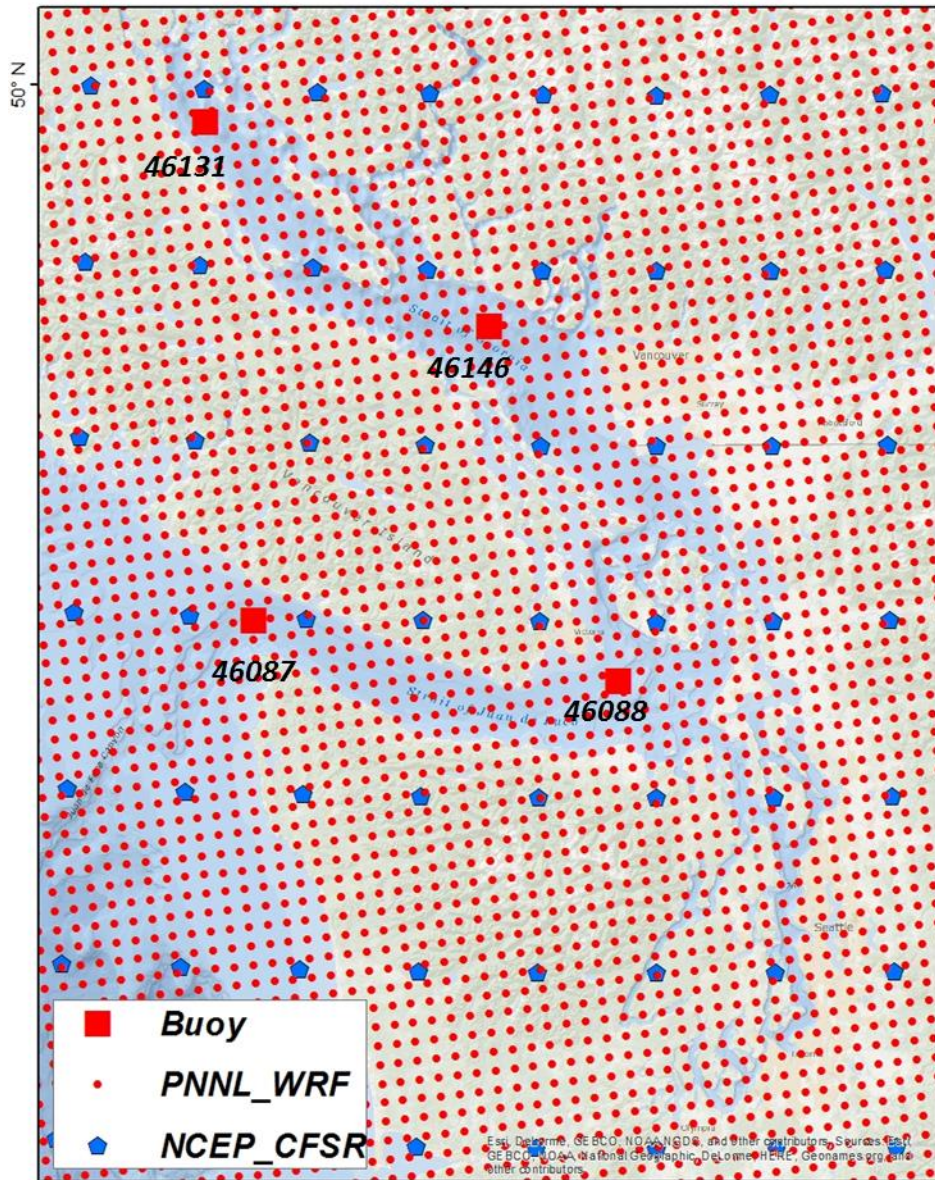


**Figure 3.** Comparison of NOAA NCEP CFSR and PNNL WRF model grid resolutions. The red squares are locations of wave buoys for model validation.

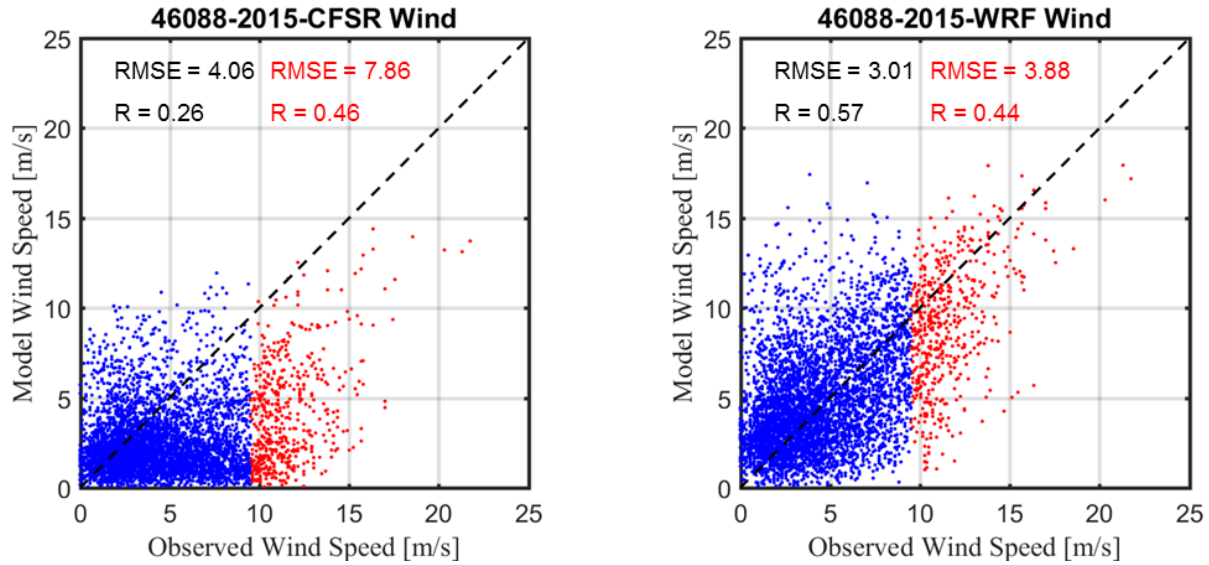


**Figure 4.** Scatter plots of hourly (a) CFSR wind and (b) WRF wind against observed data at Buoy 46088 in the eastern Strait of Juan de Fuca. Red dots indicate the data points of the top 10% wind speed.

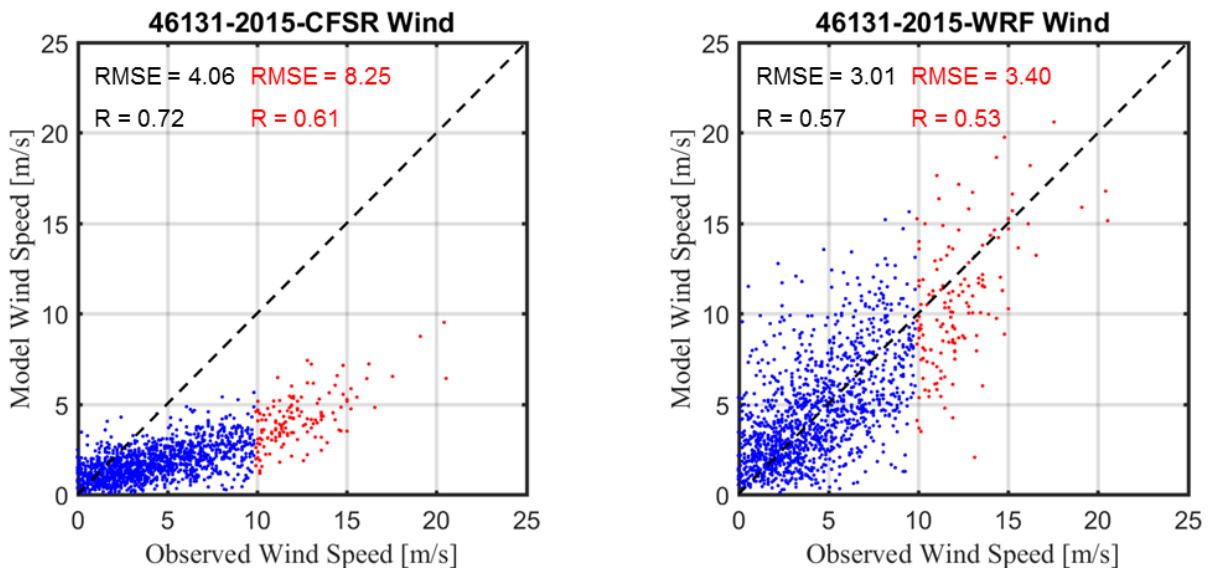


**Figure 5.** Scatter plots of hourly (a) CFSR wind and (b) WRF wind against observed data at Buoy 46131, in the northern Georgia Strait. Red dots indicate the data points of top 10% wind speed.

### 2.3 Simulation Period

Although long-term wind data from CFSR and PNNL WRF are available, only five-year simulations, from 2011 to 2015, were conducted in this study due to the constraints of time and resources. Comparison of wave climate at National Data Buoy Center Buoy 46087 and 46088 (Figure 6) in the Strait of Juan de Fuca, for the simulation period (2011–2015) and the entire data record (2004–2017) indicates that the long-term wave climate can be reasonably represented by the wave climate for the period of 2011–2015. Therefore, the 5-year UnSWAN simulation (2011–2015) is adequate for purpose of this study.

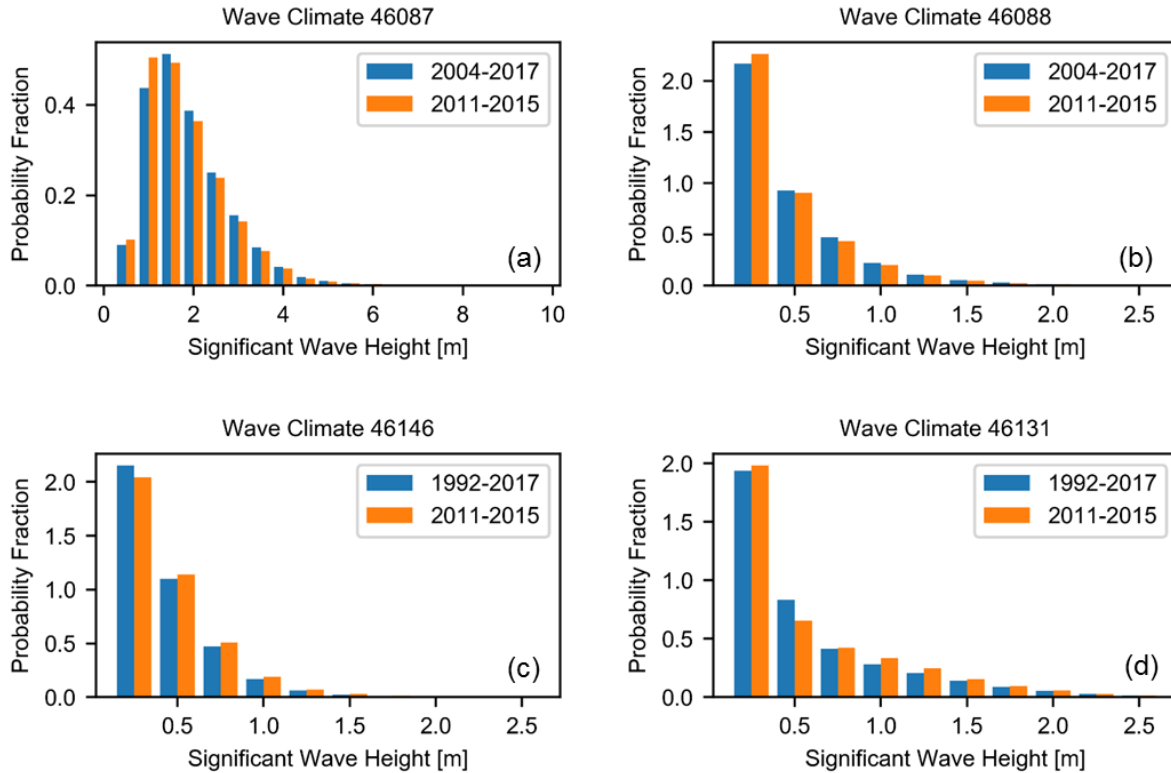


**Figure 6.** Comparison of the hourly wave climate at Buoys 46087 (a), 46088 (b), 46146 (c), and 46131 (d) for the simulation period (2011–2015) and data record period.

### 3.0 Model Results

#### 3.1 Model Validation – Time History

Model validation is a critical step in numerical modeling, especially when a model is developed for the purpose of real-world applications. Wave measurements are very limited in the Salish Sea. Wave measurements at four buoy stations inside the Salish Sea (Figure 3) are available for model validation for the period of 2011–2015. Comparisons of significant wave height for 2015 at all four buoy stations are shown in Figure 7 and Figure 8. The results for years 2011 to 2014 are similar to those for 2015. Figure 7 and Figure 8 show that the overall model results match the observed data very well. The model captured the seasonal variation as observed in the data; large waves were present in the winter and calm seas in the summer. It is also interesting to see how the seasonality of wave climate changes in the straits, as shown in Figure 7 **Error! Reference source not found.**. At the entrance of the Strait of Juan de Fuca (Buoy 6087), long-period large waves are dominant during the winter, while on the eastern side of the strait (Buoy 46088), short-period waves are dominant, especially in the summer. On the other hand, the wave climate in the southern Strait of Georgia (Buoy 46146) is somewhat similar to that in the eastern Strait of Juan de Fuca, with short-period waves dominant in the summer. In the northern Strait of Georgia (Buoy 46131), long-period large waves become dominant during winter.

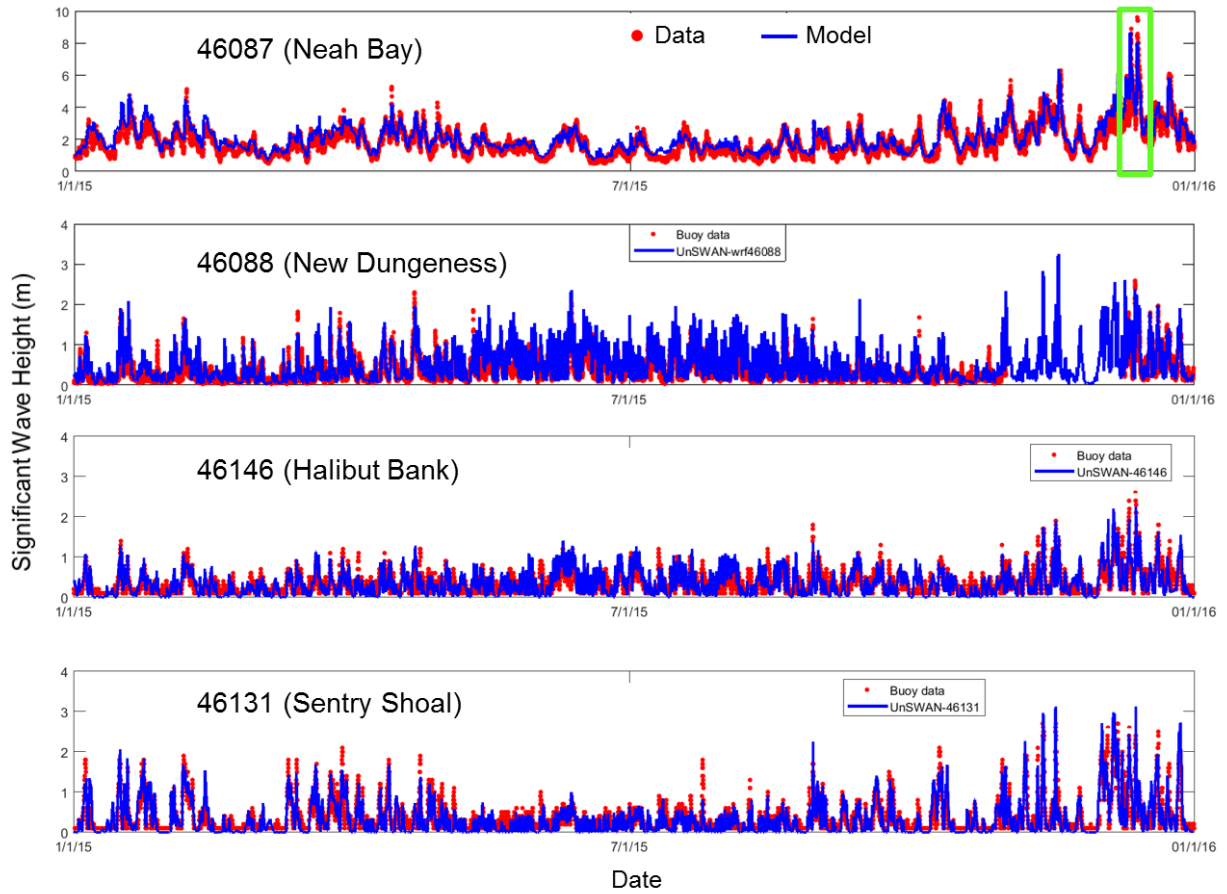


**Figure 7.** Comparison of simulated and measured hourly significant wave height at Buoys 46087 and 46088 in the Strait of Juan de Fuca and Buoys 46146 and 46131 in the Georgia Strait for 2015.



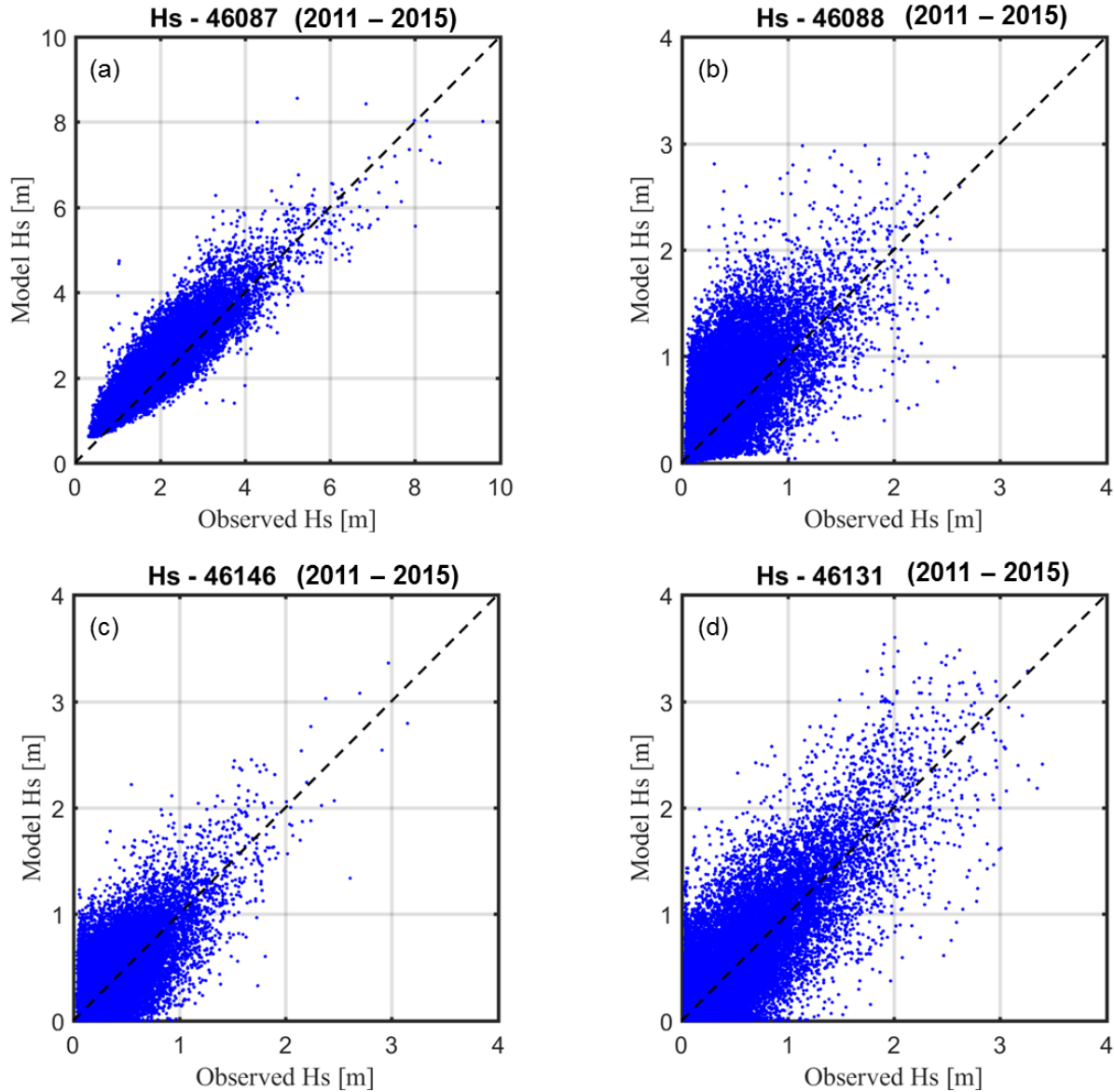


**Figure 8.** Scatter plots of modeled and observed significant wave heights at hourly intervals at Buoy 46087 (a), 46088 (b), 46146 (c), and 46131 (d) for the period of 2011–2015

The quality of peak wave direction data was very poor at all buoy stations, so no comparisons to the model results were made. Peak wave period data at Buoys 46131 and 46146 were also poor so only comparisons for peak wave period were made at Buoys 46087 and 46088 (Figure 9 and Figure 10). At Buoy 46087, wave periods were generally longer (7–20 seconds), indicating dominant long-period swell propagating from the outer coast. In contrast, peak wave periods at Buoy 46088 were smaller than those at Buoy 46087; they had a range of 2–15 seconds. The lower bound of 2 seconds is likely due to the cut-off frequency of 0.505 Hz in the model configuration. Overall, model-predicted peak wave period was comparable to the measured data, especially in capturing the distribution patterns at both buoy stations.

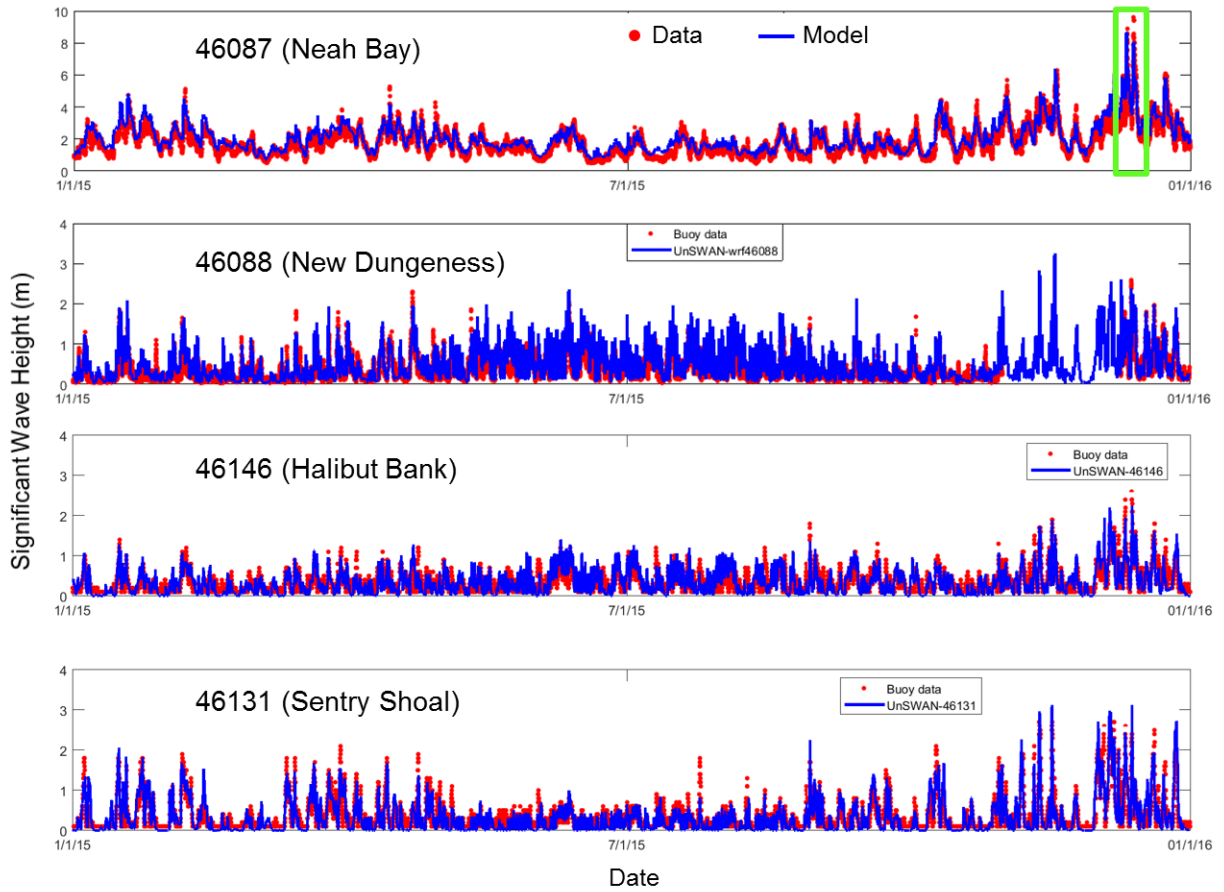


**Figure 9.** Comparison of simulated and measured peak period at Buoys 46087 and 46088 for 2015.

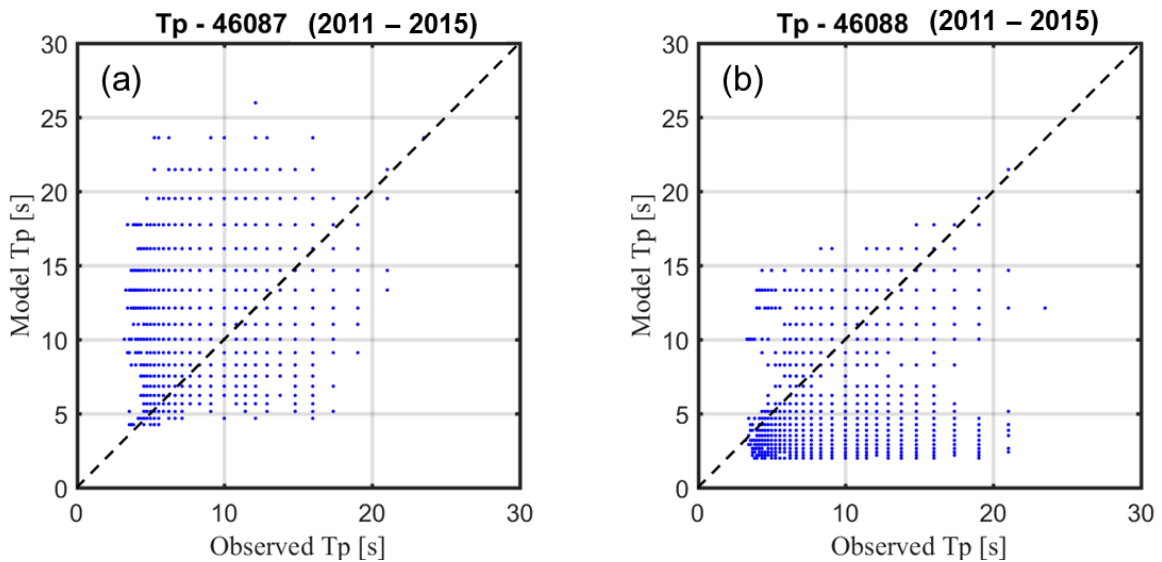


**Figure 10.** Scatter plots of modeled and observed wave peak period at hourly intervals at Buoys 46087 (a) and 46088 (b) for the period of 2011–2015.

### 3.2 Model Validation – Error Statistics

Five error statistics parameters were calculated to quantify the model performance (model skill) in reproducing the observed wave climate in the Salish Sea. As above, these comparisons were performed at a hourly intervals. The five parameters included the root-mean-square-error (*RMSE*), percent error (*PE*), scatter index (*SI*), bias, and linear correlation coefficient (*R*). The error statistics are provided in Table 3.1. These error statistic values for model validation are comparable to other modeling studies for other regions (García-Medina et al. 2014; Robertson et al. 2014; Yang et al. 2017). The formulations of these parameters are provided in Appendix A.

**Table 3.1.** Error statistics of simulated  $H_s$  and  $T_p$ .

Parameter	Buoy	RMSE	SI	PE (%)	Bias	R
$H_s$ [m]	46041	0.27	0.23	20.4	0.27	0.94
	46087	0.47	0.26	20.1	0.26	0.91
	46088	0.35	0.89	67.8	0.15	0.69
	46131	0.27	0.73	22.5	0.04	0.86
	46146	0.24	0.68	21.5	0.01	0.73
$T_p$ [s]	46041	1.45	0.21	16.3	1.11	0.86
	46087	1.32	0.18	11.4	0.78	0.79
	46088	1.97	0.52	4.3	0.06	0.23

### 3.3 Wave Climate

Figure 11 shows the instantaneous distribution of significant wave height on December 11, 2015, during a storm event, for the entire model domain. Clearly, large waves dissipated quickly as they propagated into the Salish Sea. The wave heights shown in Figure 9 are large because the map shows the deep water wave height. Although the exact height depends on shoreline conditions, waves reaching the shoreline would be much smaller than what is shown here.

Wave heights inside Puget Sound are generally much smaller than on the outer coast. However, wave heights gradually increase toward the north in the Strait of Georgia, due to wind blowing from the south. To compare the difference of wave climate in Puget Sound versus the Pacific coast, time histories of significant wave heights at Seattle and Neah Bay (entrance to the Strait of Juan de Fuca) were plotted in Figure 12. Significant wave height in Seattle is significantly smaller than that at the outer coast during a storm event, indicating Puget Sound is sheltered from large wave action, especially from waves that are propagating from the Pacific Ocean.



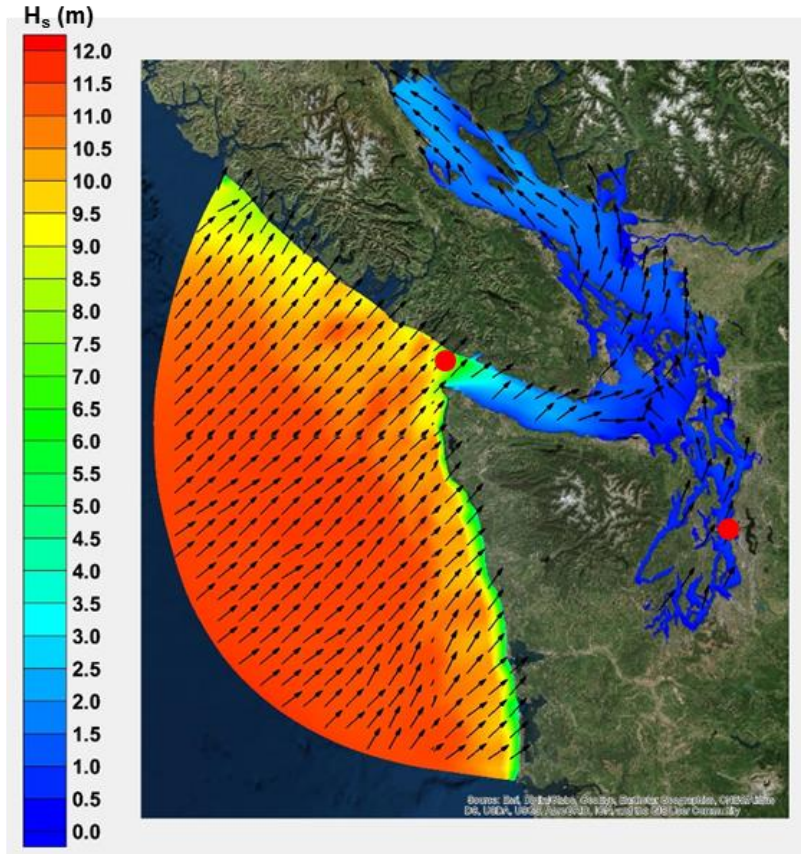


**Figure 11.** Distribution of significant wave height on December 11, 2015. The arrow represents the wind direction. The two red dots are locations for the wave height comparison shown in Figure 12.

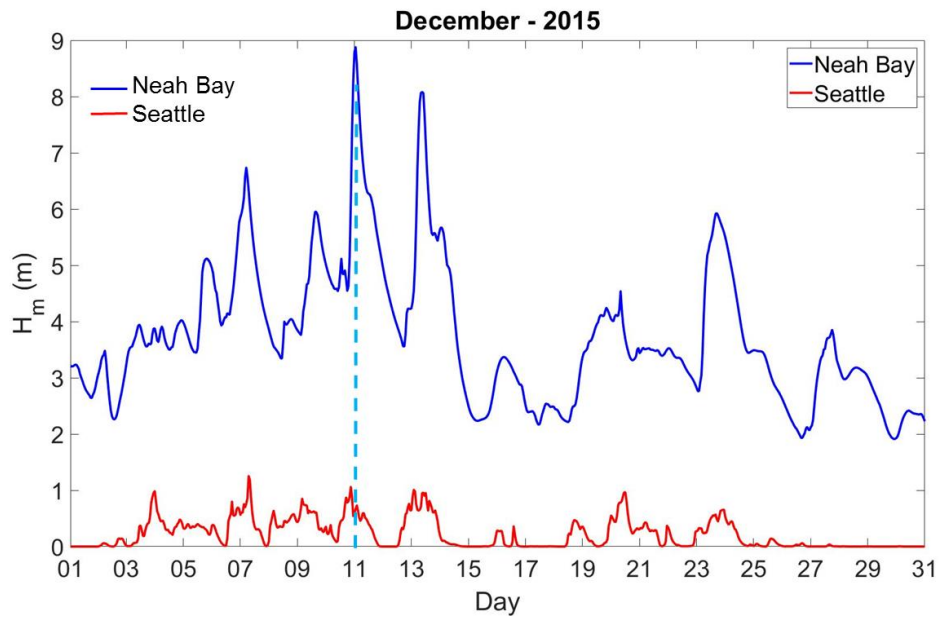


**Figure 12.** Comparison of significant wave height at Neah Bay and Seattle. The blue dashed line indicates the time of the horizontal distribution shown in Figure 11.

Simulated significant wave height ( $H_s$ ), peak wave period ( $T_p$ ), and peak wave direction ( $D_p$ ) in the entire model domain were analyzed for the period of 2011–2015. The top 1%  $H_s$  value and the corresponding  $T_p$  were extracted and plotted in Figure 13. Figure 13 shows that wave height and peak period in the Straits are greater than those inside Puget Sound, although they are much smaller than those on the Pacific Northwest coast. The data file format is included in Appendix B.

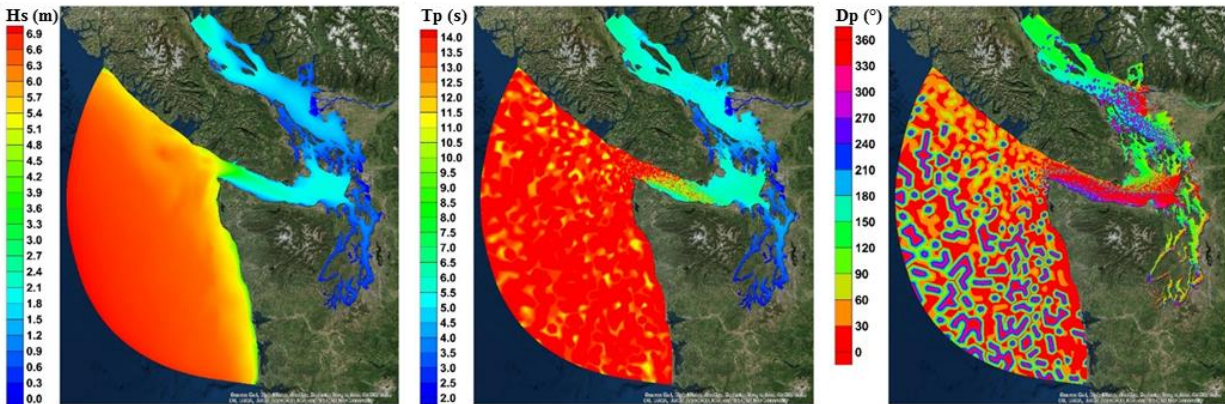


**Figure 13.** Simulated 1% significant wave height (a) and corresponding peak period (b) and direction (c) based on hourly output of five years of simulation (2011–2015).

## 4.0 Summary

A high-resolution wave modeling study using unstructured-grid SWAN was conducted to simulate the wave climate in the Salish Sea. The UnSWAN model was driven by the three-level nested global-regional WWIII model output and high-resolution WRF wind. The model was validated with available wave data inside the Salish Sea and good agreement between model results and observed data were achieved. Model performance error statistics were calculated and showed good model skill in reproducing the wave climate at the buoy stations. The good model validation demonstrates that the Salish Sea wave model has the capability of simulating the wave climate in the Salish Sea and therefore can be used to generate useful information to support coastal risk management in the region.

The model output of the top percentiles (i.e., 5%, 1%, and 0.1%) of hourly significant wave height and the corresponding peak period and direction during the high wave events was calculated based on the model simulation and delivered to the Climate Impact Group of the University of Washington.

## 5.0 References

EPRI (Electric Power Research Institute). 2011. Mapping and Assessment of the U.S.s Ocean Wave Energy Resource. Technical Report to the U.S. Department of Energy, Palo Alto, California.

Gao Y, LR Leung, C Zhao, and S Hagos. 2017. "Sensitivity of U.S. summer precipitation to model resolution and convective parameterizations across gray zone resolutions." *Journal of Geophysical Research-Atmospheres* 122, doi:10.1002/2016JD025896.

García-Medina G, HT Özkan-Haller, and P Ruggiero. 2014. "Wave resource assessment in Oregon and southwest Washington, USA." *Renewable Energy* 64:203-214.

Robertson BR, CE Hiles, and BJ Buckham. 2014. "Characterizing the near shore wave energy resource on the west coast of Vancouver Island, Canada." *Renewable Energy* 71:665-678.

Yang Z, V Neary, T Wang, B. Gunawan, A Dallman, and WC Wu. 2017. Wave resource modeling test bed study. *Renewable Energy* 114, pp. 132-144. <http://dx.doi.org/10.1016/j.renene.2016.12.057>

Yang Z, W-C Wu, T Wang, and L Castrucci. 2018. High-Resolution Regional Wave Hindcast for the U.S. West Coast. Pacific Northwest National Laboratory, Richland, Washington.



## Appendix A – Formulations of the Error Statistic Parameters

To quantitatively evaluate the model performance in simulating the wave climate five statistics were computed to compare model results with measurements. The root-mean-square-error (*RMSE*) is defined as follows:

$$RMSE = \sqrt{\frac{\sum_{i=1}^N (P_i - M_i)^2}{N}}$$

where  $N$  is the number of observations,  $M_i$  is the measured value, and  $P_i$  is the model generated value. The scatter index (*SI*) is the *RMSE* normalized by the average measurement:

$$SI = \frac{RMSE}{\bar{M}}$$

The percent error (*PE*) is defined as follows:

$$PE = 100 \sqrt{\frac{1}{N} \sum_{i=1}^N \left( \frac{P_i - M_i}{M_i} \right)^2}$$

This parameter helps put the *RMSE* values into context when comparing regions of large wave heights with regions of small wave heights. The bias is defined as follows:

$$Bias = \frac{\sum_{i=1}^N P_i - M_i}{N}$$

Finally, the linear correlation coefficient ( $R$ ) is a measure of the linear relationship between the predictions and the measurements from 0 to 1 where 1 is a perfect fit:

$$R = \frac{\sum_{i=1}^N (P_i - \bar{P})^2 (M_i - \bar{M})^2}{\sqrt{\left( \sum_{i=1}^N (M_i - \bar{M})^2 \right) \left( \sum_{i=1}^N (P_i - \bar{P})^2 \right)}}$$



## Appendix B – Data File Format

The top 5%, 1%, and 0.1%  $H_s$  value and the corresponding  $T_p$  and  $D_p$  were extracted and saved in an ASCII file (e.g., Top\_1percent\_Hs\_Tp\_Dp\_SalishSea.txt). Below is the example of the file format for the 1% output. (X, Y) are the location coordinates in NAD 1983 – UTM Zone 10 N. The file was delivered to the Climate Impact Group of the University of Washington as part of the deliverable for this project.

X	Y	Hs(m)	Tp(s)	Dp(degr)
2.4283902e+05	5.4875313e+06	3.2800000e+00	8.2740000e+00	9.8828000e+01
2.3979669e+05	5.4825912e+06	5.6910000e+00	1.1014000e+01	6.7352000e+01
2.3684034e+05	5.4774754e+06	5.7530000e+00	1.6126000e+01	2.2136000e+01
2.3398413e+05	5.4721790e+06	5.8410000e+00	1.2115000e+01	6.4608000e+01
2.3122150e+05	5.4667089e+06	5.8960000e+00	1.6126000e+01	1.4632000e+01
2.2856011e+05	5.4610638e+06	6.0650000e+00	1.4660000e+01	9.8650000e+00
2.2600654e+05	5.4552434e+06	6.1630000e+00	1.4660000e+01	6.7770000e+00
2.2356615e+05	5.4492481e+06	6.2580000e+00	1.1014000e+01	6.5825000e+01
2.2122515e+05	5.4430855e+06	6.3630000e+00	1.6126000e+01	1.1130000e+01
2.1897089e+05	5.4367617e+06	6.4390000e+00	1.7739000e+01	1.4537000e+01
2.1678983e+05	5.4302817e+06	6.5260000e+00	1.3327000e+01	3.5481200e+02
2.1468929e+05	5.4236430e+06	6.5770000e+00	1.3327000e+01	5.1831000e+01
2.1269507e+05	5.4168380e+06	6.6110000e+00	1.4660000e+01	5.4295000e+01
2.1084676e+05	5.4098568e+06	6.6460000e+00	1.3327000e+01	5.1244000e+01
2.0915772e+05	5.4026987e+06	6.6740000e+00	1.4660000e+01	5.5046000e+01



**Pacific  
Northwest**  
NATIONAL LABORATORY

***[www.pnnl.gov](http://www.pnnl.gov)***

902 Battelle Boulevard  
P.O. Box 999  
Richland, WA 99352  
1-888-375-PNNL (7665)

---

U.S. DEPARTMENT OF  
**ENERGY**